CHEMISTRY
A EUROPEAN JOURNAL

DOI: 10.1002/chem.200501097

Mechanistic Insight into the Activity of Tyrosinase from Variable-Temperature Studies in an Aqueous/Organic Solvent

Alessandro Granata,[a] Enrico Monzani,[a] Luigi Bubacco,[b] and Luigi Casella*[a]

Abstract: The activity of mushroom tyrosinase towards a representative series of phenolic and diphenolic substrates structurally related to tyrosine has been investigated in a mixed solvent of 34.4% methanol–glycerol (7:1, v/v) and 65.6% (v/v) aqueous 50 mM Hepes buffer at pH 6.8 at various temperatures. The kinetic activation parameters controlling the enzymatic reactions and the thermodynamic parameters associated with the process of substrate binding to the enzyme active species have been deduced from the temperature variation of the k_{cat} and K_M parameters. The activation free energy is dominated by the enthalpic term, the value of which lies in the relatively narrow range of 61 ± 9 kJ mol^{-1} irrespective of substrate or reaction type (monophenolase or diphenolase). The activation entropies are small and generally negative and contribute no more than 10% to the activation free energy. The substrate binding parameters are characterized by large and negative enthalpy and entropy contributions, which are typically dictated by polar protein–substrate interactions. The substrate 4-hydroxyphenylpropionic acid exhibits a strikingly anomalous temperature dependence of the enzymatic oxidation rate, with $\Delta H^{\neq} \approx 150$ kJ mol^{-1} and $\Delta S^{\neq} \approx 280$ J K^{-1} mol^{-1}, due to the fact that it can competitively bind to the enzyme through the phenol group, like the other substrates, or the carboxylate group, like carboxylic acid inhibitors. A kinetic model that takes into account the dual substrate/inhibitor nature of this compound enables rationalization of this anomalous behavior.

Keywords: activation parameters · bioinorganic chemistry · enzymes · thermodynamic parameters · tyrosinase

Introduction

Tyrosinase (EC 1.14.18.1) is a copper monooxygenase that catalyzes the *ortho*-hydroxylation of monophenols (monophenolase activity) and the oxidation of catechols (diphenolase activity) to *ortho*-quinones according to the stoichiometries given in Equations (1) and (2).[1]

(1)

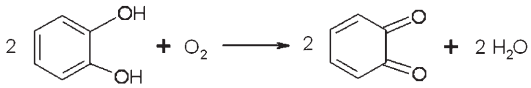

(2)

The monophenolase reaction is often shown to proceed through the initial formation of catechol followed by oxidation to quinone,[2] but this point is still subject to considerable debate as in vitro catechol is probably formed by way of an indirect nonenzymatic mechanism.[3] The active site of the enzyme contains a pair of antiferromagnetically coupled copper(II) ions in the met form, and during turnover both the reduced and the oxy forms are cyclically produced.[4] The structure of tyrosinase is not known, but evolutionary correlations[5] and spectroscopic similarities[6] with two closely related proteins belonging to the same type-3 copper family that have been structurally characterized, namely hemocyanin[7,8] and catechol oxidase,[9] suggest a common active site, in which six histidine ligands are bound to the pair of copper ions. A direct indication of the presence of six coordinating histidines in tyrosinase comes from paramagnetic NMR experiments on the enzyme from *Streptomyces antibioticus*.[10] Differences in the function of type-3

[a] Dr. A. Granata, Dr. E. Monzani, Prof. L. Casella
Dipartimento di Chimica Generale, Università di Pavia
Via Taramelli 12, 27100 Pavia (Italy)
Fax: (+39) 0382-528-544
E-mail: bioinorg@unipv.it

[b] Prof. L. Bubacco
Dipartimento di Biologia, Università di Padova
30121 Padova (Italy)

Supporting information (the derivation of the rate equation and the activation parameters for the enzymatic reaction involving a substrate with two binding modes, and the kinetic parameters and rate plots for the enzymatic oxidation of all of the phenolic and diphenolic substrates at variable temperatures) for this article is available on the WWW under http://www.chemeurj.org/ or from the author.

copper proteins seem to largely depend on the accessibility of the dioxygen binding site to potential substrates and selectivity effects that discriminate the type of substrates. Thus, while the active site of hemocyanins is basically inaccessible except to small ligand molecules, proteolytic or sodium dodecyl sulfate (SDS) activation of the protein can induce mono- and diphenolase activity.[11,12] Catechol oxidases are normally only able to catalyze the diphenolase reaction [Eq. (2)], and are inactive, or only very weakly active, with monophenols.[13]

Despite extensive research efforts, very little is known about the details of the mechanisms through which tyrosinase catalyzes reactions according to Equation (1) and Equation (2). The mode of substrate binding at the enzyme and product release therefrom, and the mode of dioxygen activation and cleavage at the dicopper center are, in particular, completely unknown.[14,15] Although the monophenolase reaction [Eq. (1)] involves the energetically demanding step of oxygen atom insertion into the aromatic C–H bond, the monophenolase catalytic cycle is simpler than the diphenolase cycle. In fact, only the oxy form of tyrosinase is able to carry out the phenol hydroxylation, while catechols are oxidized both by the met form and the oxy form of the enzyme. A simplified view of the commonly accepted steps involved in these mechanisms is provided in Scheme 1 and

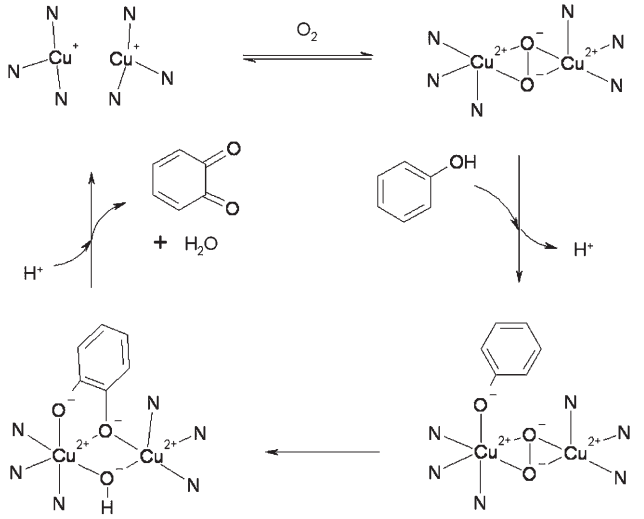

Scheme 1.

Scheme 2. In these schemes, binding of catechol to met-tyrosinase has been represented to occur in the η^2:η^1 bridging mode, rather than the commonly adopted μ-1,4 bridging mode.[4] The asymmetric η^2:η^1 binding mode is suggested by collective evidence from inhibitor binding studies to half-met[16] and met[17] *Streptomyces antibioticus* tyrosinase, spectroscopic studies on biomimetic catecholate-dicopper(II) complexes,[18] and by the X-ray structure of catechol oxidase with a bound phenylthiourea inhibitor molecule.[9,13] The η^2:η^1 catechol complex has the advantage of requiring mini-

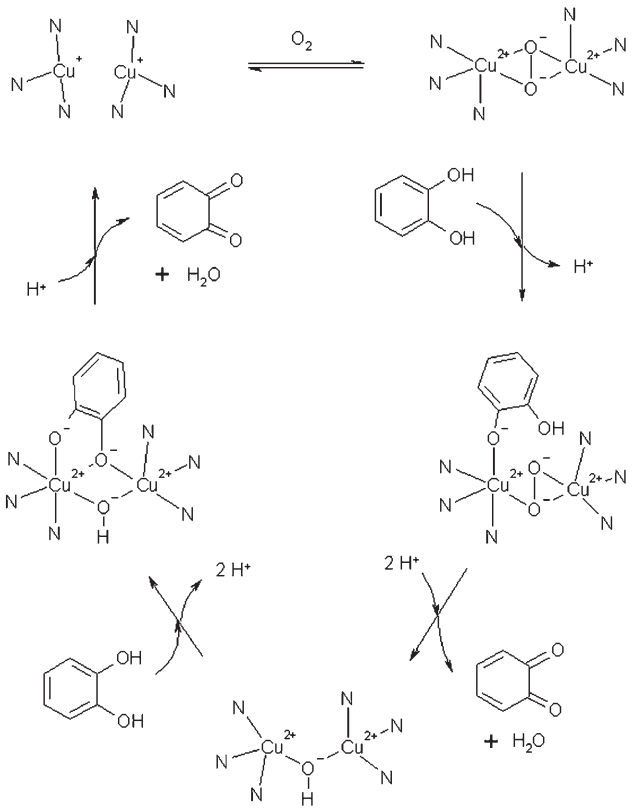

Scheme 2.

mal steric rearrangement in the step involving evolution of the phenolate–peroxy intermediate in the monophenolase cycle of Scheme 1. The two catalytic cycles of tyrosinase are usually shown intermingled, due to the fact that in vitro the monophenolase reaction typically exhibits a lag phase that no longer occurs on the addition of limited amounts of a diphenol, the function of which is to reduce met tyrosinase, the major component of the enzyme as isolated, and give rapid access to the oxy form.[3]

A recent theoretical calculation performed on the monophenolase reaction [Eq. (1)] indicates that the rate-limiting step is associated with cleavage of the peroxide O–O bond (60.2 kJ mol^{-1}), but the attack of peroxide on the phenolate ring is also characterized by a significant energy barrier (51.5 kJ mol^{-1}).[15] A different conclusion has been reached on the basis of kinetic investigations, according to which the rate-limiting step is connected with phenol deprotonation and binding to the copper–peroxo intermediate.[19,20] Indeed, both tyrosinase catalytic cycles involve proton transfer steps and, in particular, the phenol has been suggested to transfer a proton to the peroxo group.[21]

In the present study, we report an investigation of the activity of mushroom tyrosinase towards a group of representative substrates related to tyrosine (Figure 1) over a range of temperatures in a mixed aqueous/organic solvent. In this medium, which enables an extension of the range of temperatures normally accessible in aqueous buffer, we have ob-

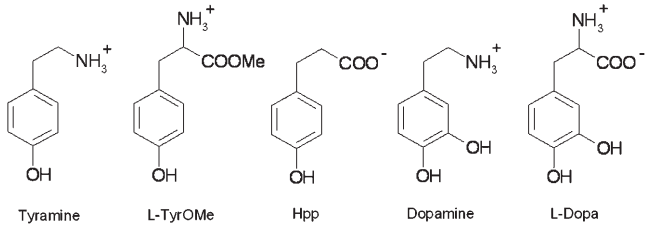

Figure 1. Structures of the phenolic substrates employed in the kinetic studies.

tained the thermodynamic and activation parameters associated with the rate-limiting step of the enzymatic reactions.

Results

In preliminary investigations, the enzymatic activity of tyrosinase was tested in a variety of mixed aqueous/organic solvents having suitable viscosity characteristics for use as cryosolvents in low-temperature studies.[22] Among these media, mixtures composed of methanol–glycerol (7:1, v/v) as organic component and aqueous Hepes buffer at pH 6.8 were found to facilitate good performance of the enzyme. As we were not interested in attaining very low temperatures in the present study, we maintained a relatively large fraction of aqueous buffer. Thus, using a ratio of 34.4% methanol–glycerol (7:1, v/v) and 65.6% (v/v) aqueous 50 mM Hepes buffer at pH 6.8, we found very good operation of the enzyme in the temperature range of -20 to $+30$ °C. The effect of the cryosolvent on enzyme activity was assessed using L-Dopa as substrate. A very weak, mixed-type inhibition effect was found by studying the dependence of the rate of L-Dopa oxidation as a function of the concentration of the organic component of the cryosolvent (data not shown). These weak solvent effects could therefore be neglected in the treatment of kinetic data for the substrates investigated.

Addition of the organic component to the aqueous buffer has the drawback of limiting the solubility of the natural phenolic substrates containing charged groups in their side chains, and for this reason we could not investigate the behavior of L-tyrosine over an extended concentration range. However, a number of physiologically relevant tyrosine derivatives, namely tyramine, L-TyrOMe, 4-hydroxyphenylpropionic acid (Hpp), dopamine, and L-Dopa, exhibited sufficient solubility in the cryosolvent to enable a detailed enzymatic study over a suitable range of temperatures. The enzymatic oxidation of *N*-acetyl-L-tyrosine was also investigated, but it was found to be extremely slow in the cryosolvent, as it is in aqueous buffer.[23]

In Table 1, the kinetic parameters of the enzyme in our selected aqueous/organic solvent are compared with literature data relating to aqueous buffer at the same pH. A further comparison between results obtained at 10 °C and 25 °C allows consideration of the effect of temperature on the kinetic parameters. The activity of tyrosinase in the cryosolvent is slightly decreased or slightly increased with respect to that in aqueous buffer, depending on the substrate, but the effect on k_{cat} is generally accompanied by an increase of K_M, so that the efficiency of the enzyme is somewhat decreased in the aqueous/organic medium. The abrupt drop in k_{cat} at the lower temperature for Hpp is, however, worthy of note. In all cases, the turnover rates were found to be independent of $[O_2]$. This is expected, in view of the higher solubility of dioxygen in the organic medium with respect to water[24] and considering the high value of the rate constant for binding of O_2 to deoxy tyrosinase.[25] In order to probe the existence or otherwise of an isotope effect for the monophenolase reaction in the mixed solvent, the activities of the enzyme towards 3,5-$[D_2]$-L-TyrOMe and L-TyrOMe were compared (Figure 2).

Table 1. Comparison of the kinetic parameters for the activity of tyrosinase in the mixed solvent of 34.4% methanol–glycerol (7:1, v/v) and 65.6% (v/v) aqueous 50 mM Hepes buffer pH 6.8, and in 50 mM phosphate buffer pH 6.8.[a]

Solvent[b]/T [°C]	Parameter	Tyramine	L-TyrOMe	Hpp[c]	Dopamine	L-Dopa
C/25	k_{cat} [s^{-1}]	7.4 ± 0.2	8.9 ± 0.1	43.0 ± 2.0	133.2 ± 1.2	141.1 ± 3.0
	K_M [mM]	2.1 ± 0.1	0.82 ± 0.04	6.7 ± 0.4	0.93 ± 0.02	3.7 ± 0.2
C/10	k_{cat} [s^{-1}]	1.90 ± 0.05	2.24 ± 0.08	1.70 ± 0.04	29.9 ± 0.4	42.0 ± 1.0
	K_M [mM]	0.66 ± 0.05	0.28 ± 0.03	0.22 ± 0.02	0.40 ± 0.01	2.1 ± 0.1
A/25	k_{cat} [s^{-1}]	25.9 ± 1.1	3.4 ± 0.14[d]	66.7 ± 2.7	439 ± 17.6	107.4 ± 3.1
	K_M [mM]	0.51 ± 0.02	0.38 ± 0.04[d]	0.44 ± 0.01	2.2 ± 0.1	0.8 ± 0.03

[a] Data taken from reference [19]. [b] C = cryosolvent, A = aqueous buffer. [c] k_{cat} and K_M values reported for Hpp are the apparent values obtained from simple Michaelis–Menten treatment. [d] Taken from: L. G. Fenoll, J. N. Rodriguez-Lopez, F. Garcia-Molina, F. Garcia-Canovas, J. Tudela, *Int. J. Biochem. Cell Biol.* **2002**, *34*, 332–336.

The kinetic parameters $k_{cat} = 5.57\pm0.04\ s^{-1}$ and $K_M = 0.61\pm0.04$ mM obtained for 3,5-$[D_2]$-L-TyrOMe at 20 °C are similar to those for L-TyrOMe ($k_{cat} = 5.97\pm0.08\ s^{-1}$, $K_M = 0.58\pm0.02$ mM), but indicate a small but non-negligible isotope effect on the rate constant ($k_{cat}^H/k_{cat}^D = 1.1$) in the mixed aqueous/organic solvent. The isotope effect was found to be unchanged by repeating the measurements at 15 °C and 25 °C ($k_{cat}^H/k_{cat}^D = 1.1\pm0.05$). This is in contrast with the absence of isotope effect found for the enzymatic oxidation of *p*-chlorophenol using hydrogen peroxide instead of dioxygen as oxidant in 0.5 M aqueous borate buffer at pH 7.0.[26]

The initial rates for the enzymatic oxidation of phenolic and diphenolic substrates were measured as a function of substrate concentration at various temperatures in the cryosolvent. A representative family of curves obtained for L-Dopa is shown in Figure 3.

A complete list of kinetic parameters at various temperatures along with the corresponding rate plots for all of the substrates investigated is provided in the Supporting Materi-

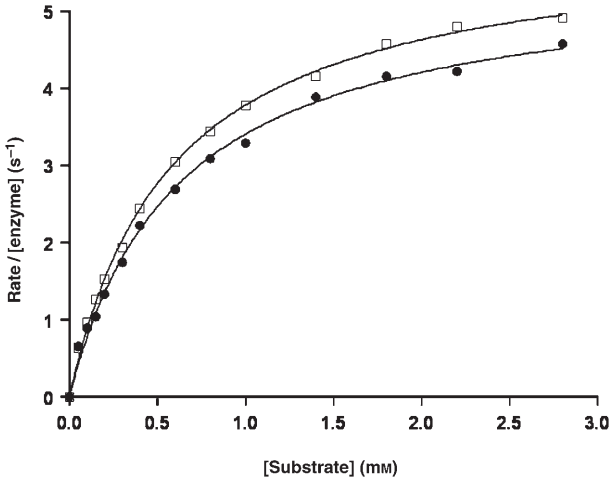

Figure 2. Rate dependence on substrate concentration, at 20 °C, for the catalytic oxidation of L-TyrOMe (□) and 3,5-[D_2]-L-TyrOMe (●) by tyrosinase in the mixed solvent of 34.4 % methanol–glycerol (7:1) and 65.6 % aqueous Hepes buffer (50 mM) at pH 6.8.

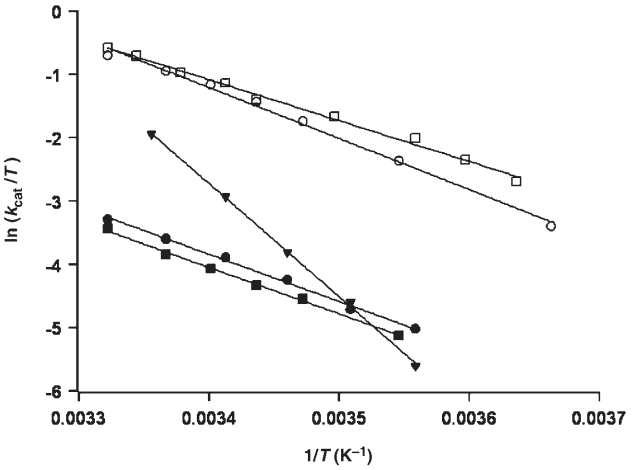

Figure 4. Eyring plots for the tyrosinase-catalyzed oxidation of L-Dopa (□), dopamine (○), tyramine (■), L-TyrOMe (●), and Hpp (▼) in the mixed solvent of 34.4 % methanol–glycerol (7:1) and 65.6 % aqueous Hepes buffer (50 mM) at pH 6.8.

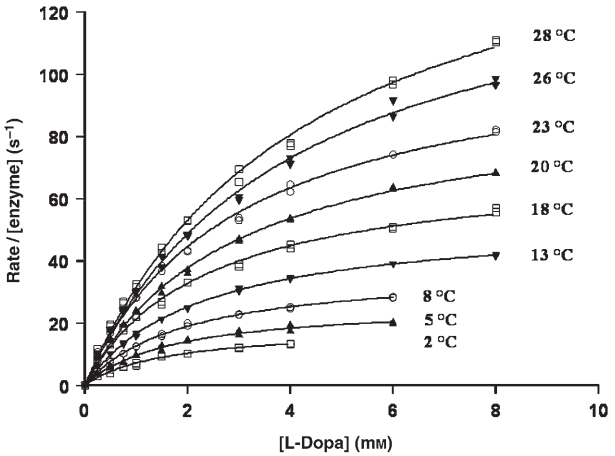

Figure 3. Rate dependence on substrate concentration at different temperatures of the oxidation of L-Dopa by tyrosinase in the mixed solvent of 34.4 % methanol–glycerol (7:1) and 65.6 % aqueous Hepes buffer (50 mM) at pH 6.8.

al. Eyring plots of $\ln k_{cat}/T$ against T^{-1} yielded the activation parameters $\Delta H^{\neq}$ and $\Delta S^{\neq}$; these are shown in Figure 4 for all of the substrates.

The temperature range investigated for each substrate was defined by the reduced stability and inactivation of the protein at high temperature and by the very low activity as the temperature approaches 0 °C. The latter problem proved to be especially relevant with the phenolic substrates, since the lag phase was considerably extended at low temperature and did not allow the determination of reliable kinetic data below about 8 °C. In any case, the temperature range analyzed, up to about 30 °C, ensures a constant enthalpy contribution. The k_{cat} values at 25 °C were used to calculate the activation free energy $\Delta G^{\neq}$ for the enzymatic reactions at this temperature (Table 2). It can be seen from Table 2 that the $\Delta H^{\neq}$ values fall in the relatively narrow range of 61 ± 9 kJ mol^{-1} for all the substrates bearing an amino substituent on the side chain attached to the aromatic nucleus, but that the activation enthalpy increases dramatically to about 150 kJ mol^{-1} for Hpp. Interestingly, dopamine has a significantly larger $\Delta H^{\neq}$ value than that in the case of L-Dopa. This is consistent with the more pronounced rate dependence on temperature for the former substrate. Also, $\Delta S^{\neq}$ values are small and negative for tyramine, L-TyrOMe, and L-Dopa, but this parameter becomes small and positive for dopamine and large and positive for Hpp. This is important because the entropic term significantly reduces the enthalpic contribution to $\Delta G^{\neq}$ for the latter two substrates (especially for Hpp) at room

Table 2. Activation parameters for tyrosinase activity and thermodynamic parameters for substrate binding in the mixed solvent of 34.4 % methanol–glycerol (7:1, v/v) and 65.6 % (v/v) aqueous 50 mM Hepes buffer pH 6.8 and in 50 mM phosphate buffer at pH 6.8.

Parameter/Substrate	Tyramine	L-TyrOMe	Hpp[c]	Dopamine	L-Dopa
$\Delta H^{\neq}$ [kJ mol^{-1}]	+60.9 ± 1.5	+61.9 ± 2.0	+148.6 ± 2.6	+67.1 ± 2.2	+53.8 ± 1.6
$\Delta S^{\neq}$ [J K^{-1} mol^{-1}]	−24 ± 5	−19 ± 11	+281 ± 8	21 ± 7	−23 ± 6
$\Delta G^{\neq}$ [kJ mol^{-1}] (25 °C)[a]	68.1	67.5	64.9	60.8	60.7
$\Delta H°$ [kJ mol^{-1}]	−55.1 ± 4.7	−52.4 ± 2.8	−157.2 ± 4.0	−39.6 ± 2.2	−26.8 ± 1.2
$\Delta S°$ [J K^{-1} mol^{-1}]	−134 ± 16	−117 ± 10	−485 ± 12	−75 ± 7	−43 ± 4
$\Delta G°$ [kJ mol^{-1}] (25 °C)[b]	−15.3	−17.6	−12.4	−17.3	−13.9
$\Delta H^{\neq}_{on}$ [kJ mol^{-1}][d]	5.8 ± 3.5	9.5 ± 1.8	−9 ± 8	27.5 ± 1.6	27.0 ± 1.2
$\Delta S^{\neq}_{on}$ [J K^{-1} mol^{-1}][d]	−158 ± 12	−136 ± 6	−204 ± 30	−54 ± 5	−66 ± 8
$\Delta G^{\neq}_{on}$ [kJ mol^{-1}] (25 °C)[b,d]	53	50	52	44	47

[a] Calculated from k_{cat} values at 25 °C. [b] Calculated from K_M^{-1} values at 25 °C. [c] The parameters obtained for Hpp are apparent values affected by the inhibition process. [d] The activation parameters for substrate binding are valid in the hypothesis of slow substrate dissociation from the enzyme ($k_{cat} \gg k_{off}$).

temperature. The Eyring plots clearly show the anomalous behavior of Hpp with respect to the other substrates (Figure 4). Except in the case of Hpp, the $\Delta G^{\neq}$ values are essentially determined by $\Delta H^{\neq}$, with entropy contributions restricted to no more than $\pm 10\,\%$.

In the approximation of a fast substrate binding process (see Supporting Information), the K_M^{-1} values are the apparent association constants of the substrates to the enzyme-active species. Plots of $\ln K_M^{-1}$ against T^{-1} were constructed and used to calculate $\Delta H°$ and $\Delta S°$, the enthalpy and entropy changes, respectively, associated with the formation of the enzyme-substrate complex in the steady state (Figure 5).

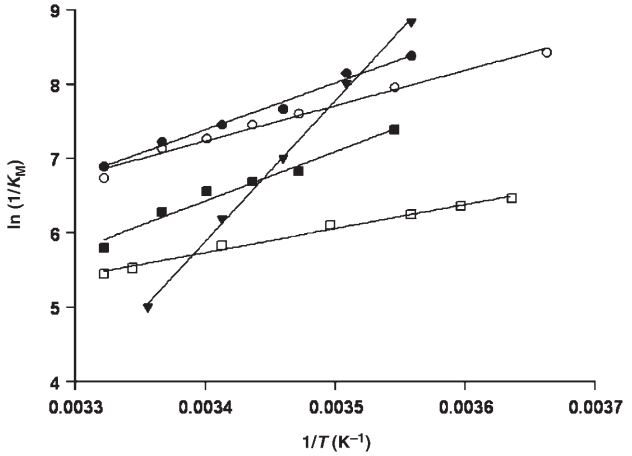

Figure 5. Van't Hoff plots for the tyrosinase-catalyzed oxidation of L-Dopa (□), dopamine (○), tyramine (■), L-TyrOMe (●), and Hpp (▼) in the mixed solvent of 34.4 % methanol–glycerol (7:1) and 65.6 % aqueous Hepes buffer (50 mM) at pH 6.8.

The values of these thermodynamic parameters, together with the $\Delta G°$ values calculated from the K_M^{-1} values at 25 °C, are collected in Table 2. The enthalpic and entropic contributions to the binding energies of the substrates are somewhat scattered, reflecting specific effects involving the polar substituents on the side chains, but in general both terms are large and negative. A similar trend in the enthalpy and entropy terms was noted previously for the binding of aromatic acid inhibitors to tyrosinase[21] and of simple phenolic compounds to heme peroxidases.[27,28] Notably, both the $\Delta H°$ and $\Delta S°$ parameters show larger negative values with phenols than with catechols.

The strikingly anomalous temperature dependence of the catalytic reaction of Hpp stems only from the presence of a carboxylate group on the side chain of the phenol nucleus. Carboxylic acids of a variety of structural types have been shown to act as inhibitors of tyrosinase because they strongly bind to the met form of the enzyme upon displacing the peroxide from oxytyrosinase.[21,29] The case of Hpp is therefore unique, because it can act as a substrate, by binding to oxytyrosinase through the phenol group, or as an inhibitor, by displacing the peroxide like other carboxylic acids. The behavior of such a bifunctional molecule can be treated according to the simplified reaction scheme given in Equation (3).

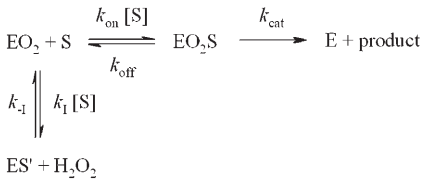

(3)

Here, S and S′ denote Hpp acting as a substrate and as an inhibitor, respectively, EO_2S is the active intermediate of the enzymatic reaction, and ES′ represents an unproductive complex. This inhibitory scheme yields the kinetic equation (4) (for its derivation, see the Supporting Information).

$$\text{rate}/[E_0] = \frac{\frac{k_{cat}}{1+K_IK_M}[S]}{\frac{K_M}{1+K_IK_M}+[S]} \quad (4)$$

Here, $K_I = k_I/k_{-I}$ is the binding constant of the inhibitor, and $K_M = (k_{cat} + k_{off})/k_{on}$. When studied as a function of substrate concentration, the rate plot shows the usual substrate saturation behavior, but with reduced maximum activity and saturation at a reduced substrate concentration. The apparent kinetic parameters deduced from these plots are related to the true parameters by the factor $1/(1 + K_IK_M)$. Therefore, the activation and thermodynamic parameters reported for Hpp in Table 2 are apparent values affected by the presence of two substrate binding modes.

To get an idea of the effect of substrate inhibition on the activation parameters, we can approximate the apparent catalytic constant as $(k_{cat})_{app} \approx k_{cat}/(K_IK_M)$. With this approximation, the apparent activation parameters are given by Equations (5) and (6),

$$\Delta H^{\neq}_{app} \approx \Delta H^{\neq} + \Delta H^{o} - \Delta H^{o}_{I} \quad (5)$$

$$\Delta S^{\neq}_{app} \approx \Delta S^{\neq} + \Delta S^{o} - \Delta S^{o}_{I} \quad (6)$$

where $\Delta H°_I$ and $\Delta S°_I$ refer to the enthalpy and entropy changes, respectively, associated with the formation of the enzyme-substrate complex in the inhibitory pathway (connected to K_I). The averages of the values of $\Delta H^{\neq}$, $\Delta S^{\neq}$, $\Delta H°$, and $\Delta S°$ obtained with tyramine and L-TyrOMe (Table 2) can be used as estimates of the corresponding values for Hpp. Assuming $\Delta H°_I$ and $\Delta S°_I$ values for Hpp similar to the thermodynamic data for the inhibition of tyrosinase activity by benzoic acid ($\Delta H°_I = -32\,\text{kcal mol}^{-1} = -134\,\text{kJ mol}^{-1}$, and $\Delta S°_I = -85\,\text{cal K}^{-1}\text{mol}^{-1} = -356\,\text{J K}^{-1}\text{mol}^{-1}$),[21] and substituting these values into the apparent activation parameters, we obtain $\Delta H^{\neq}_{app} \approx (61 - 54 + 134) = 141\,\text{kJ mol}^{-1}$ and $\Delta S^{\neq}_{app} \approx (-22 - 126 + 356) = 208\,\text{J K}^{-1}\text{mol}^{-1}$. These values are comparable with the values reported in Table 2 for Hpp and suggest that the activation energy parameters for tyrosinase activity are consis-

tent with those observed with the other phenolic substrates for this substrate as well. The same conclusion can be drawn by applying a similar treatment to the apparent Michaelis constant (data not shown). It is interesting to note that, according to Equation (4), the k_{cat}/K_M ratio is independent of the presence of two substrate binding modes. Therefore, the same should hold true for the observed activation parameters, $\Delta H^{\neq}_{obs} = \Delta H^{\neq} + \Delta H°$ and $\Delta S^{\neq}_{obs} = \Delta S^{\neq} + \Delta S°$, obtained by applying the Eyring equation to k_{cat}/K_M. The values obtained for tyramine, L-TyrOMe, and Hpp are $\Delta H^{\neq}_{obs} = 5.8 \pm 3.5$, 9.5 ± 1.8, and $-9 \pm 8\ kJ\,mol^{-1}$ and $\Delta S^{\neq}_{obs} = -158 \pm 12$, -136 ± 6, and $-204 \pm 30\ J\,K^{-1}\,mol^{-1}$, respectively. The similarity between the values for these three substrates, almost within the experimental error, shows that by taking into account the inhibition that stems from the carboxylate group, Hpp behaves like the other phenols investigated.

The analysis outlined above assumes that substrate dissociation from the enzyme–substrate complex is a fast process, that is, it is faster than substrate oxidation ($k_{cat} \ll k_{off}$). This is at variance with the hypothesis of Garcia-Canovas, according to which substrate binding is a slow equilibrium process.[30] Assuming that the latter statement is correct, the meaning of K_M changes to the ratio of the rate constants, $K_M = k_{cat}/k_{on}$ (see Supporting Information), where k_{on} is the rate constant for substrate binding to tyrosinase. The plot of $\ln K_M^{-1}$ against T^{-1} in Figure 5 then gives "observed" $\Delta H°$ and $\Delta S°$ values, which are combinations of the activation parameters for substrate binding (E + S $\rightleftarrows$ ES), $\Delta H^{\neq}_{on}$ and $\Delta S^{\neq}_{on}$, and the enzyme reaction (ES $\rightarrow$ E + product), $\Delta H^{\neq}$ and $\Delta S^{\neq}$, respectively. Interestingly, in the approximation of slow substrate binding, the ratio k_{cat}/K_M is k_{on}. Thus, the activation parameters $\Delta H^{\neq}_{on}$ and $\Delta S^{\neq}_{on}$ can be obtained by applying the Eyring equation to k_{cat}/K_M (Table 2). The large and negative values for $\Delta S^{\neq}_{on}$ are consistent with the binding process, with values mainly dependent on the nature of the phenol or diphenol substrate. Also, the $\Delta H^{\neq}_{on}$ values are different for phenols and catechols. In the case of Hpp, $\Delta H^{\neq}_{on}$ is subject to a large standard deviation, probably due to the dual character of this compound as a substrate and inhibitor.

The conversion of the ternary complex EO_2S to E and product in the monophenolase reaction [Eq. (3)], which is governed by the rate constant k_{cat}, is a composite process. It consists of the oxidation of the substrate bound at the active site to quinone and the subsequent dissociation and diffusion of the product into the bulk solution, leaving the enzyme in the dicopper(I) form. In the diphenolase reaction, the corresponding process leaves the enzyme in the dicopper(II) form. The slowest step is that controlling the value of the kinetic constant. In order to get an idea of the timescale of the processes of substrate association to the enzyme and product dissociation therefrom, the paramagnetic contribution of the protein to the ^1H NMR relaxation rates of the inhibitor kojic acid, which strongly binds to the copper(II) ions of the enzyme,[31] has been evaluated. The longitudinal relaxation times of the nuclei of the protein-bound inhibitor, T_{1b}, are related to the paramagnetic contribution to relaxation, T_{1M}, to the diamagnetic contribution to relaxation for the bound inhibitor, T_{1D}, and to the lifetime for chemical exchange, τ_M, through Equation (7).[32]

$$1/T_{1b} = 1/T_{1D} + 1/(T_{1M} + \tau_M) \quad (7)$$

Since kojic acid is bound to the copper(II) ions in the enzyme-inhibitor complex, both dipolar and contact contributions influence T_{1M}.[32] In the presence of a strong paramagnetic effect, as in the present case, the diamagnetic contribution to relaxation can be neglected. Equation (7) thus simplifies to $T_{1b} = T_{1M} + \tau_M$. The T_{1b} values obtained for the protons at the various positions of the bound inhibitor are as follows (Figure 6): proton 1, 4.6 ± 0.1 ms; proton 2, 9.9 ± 0.1 ms; protons 3, 7.4 ± 0.4 ms. The fact that the T_{1b} values for the various kojic acid protons are different indicates that T_{1b} is dominated by T_{1M}. Therefore, the lifetime for chemical exchange must be shorter than the shortest of the T_{1b} values, that is, $\tau_M < 4.6$ ms. A comparable limiting value for τ_M (< 3 ms) has been reported for the binding of *p*-nitrophenol to *S. antibioticus* met-tyrosinase.[17] The short lifetime for protein-bound kojic acid indicates a fast dissociation of this strong inhibitor from met-tyrosinase. The dissociation of quinone from the copper(I) centers of deoxy-tyrosinase, the process involved in reaction according to Equation (3), should be even faster, because copper(I) is more kinetically labile than copper(II). As the reciprocal values of k_{cat} are larger than 4.6 ms, this indicates that k_{cat} is governed by the reaction occurring at the enzyme active site and not by product dissociation.

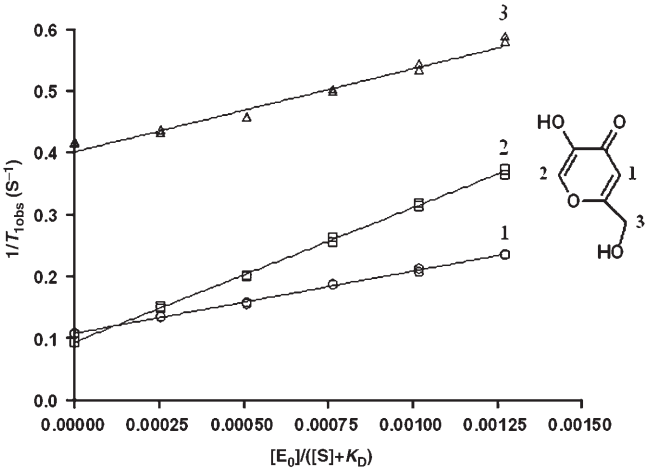

Figure 6. Dependence of the longitudinal relaxation rate ($1/T_{1obs}$) of kojic acid protons on the fraction of the inhibitor bound to the protein, $[E_0]/([S]+K_D)$. Measurements were performed in 50 mM deuterated sodium phosphate buffer, pD 6.8, containing a small amount of EDTA. The concentration of kojic acid was 10.0 mM, while that of tyrosinase ranged from 0 to 12.5 μM. The values on the plots refer to the position of the protons of kojic acid, as indicated in the inset.

Discussion

Reports on the activity of tyrosinase in organic or mixed aqueous/organic solvents have appeared previously,[33,35] although, in general, the main scope of these studies was to reduce the extent of product polymerization and enzyme deactivation. Zaks and Klibanov additionally showed that the amount of water actually required by mushroom tyrosinase to function efficiently in an organic medium is very small.[33] The present study enables us to obtain a more detailed picture of the behavior of the enzyme in the key steps of the monophenolase and diphenolase reactions. The linearity of the Eyring plots in Figure 3 indicates that there is no change in the rate-determining step of the reaction or a conformational change in the tyrosinase that affects its catalytic efficiency over the temperature range investigated. The ^{1}H NMR relaxation rate experiments performed with both kojic acid and *p*-nitrophenol[17] show that the ligand association/dissociation processes at tyrosinase are fast. Since the binding of dioxygen to deoxy-tyrosinase is very fast,[25] we can assume that the respective rate-limiting steps of the monophenolase and diphenolase reactions are represented by the processes given in Equations (8) and (9).

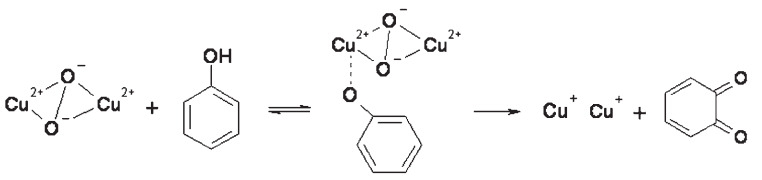

(8)

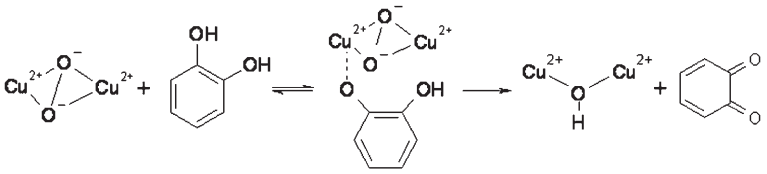

(9)

The substrates are shown to bind to copper in the deprotonated form, as is invariably assumed,[3,4,6] because a protein base, most probably a histidine,[36] assists in this process. This is confirmed by inhibition studies of tyrosinase using *p*-nitrophenol[17] and the formation of dead-end complexes between less acidic phenolic substrates and the met form of the enzyme.[19,30] Both processes depicted in Equations (8) and (9) occur with binding of the substrate to the oxy form of the enzyme, but an important difference is the release of deoxy-tyrosinase in the monophenolase reaction [Eq. (8)] and of met-tyrosinase in the diphenolase reaction [Eq. (9)]. In the catecholase cycle depicted in Scheme 2, a second molecule of catechol is oxidized by met-tyrosinase, but this reaction has been shown to be an order of magnitude faster than that of oxy-tyrosinase.[25]

The kinetic activation parameters in Table 2 thus describe the conversion of the ternary complex consisting of the enzyme, dioxygen, and substrate into the transition state. If we exclude from the comparison the anomalous case of Hpp, the data reveal clearly pronounced trends. The relative lack of dependence of $\Delta H^{\neq}$ on substrate and reaction type indicates that the key event controlling enzyme activity is common to the transition states involved in the monophenolase and catecholase reactions. This necessarily leads to the conclusion that peroxide O–O bond cleavage is the main determinant for the evolution of the transition state in both enzymatic reactions. The $\Delta H^{\neq}$ values found here (61 ± 9 kJ mol^{-1}) are consistent with theoretical calculations of the energy barrier involved in the O–O cleavage step of the monophenolase[15] and catecholase[37] reactions, even though the overall reaction mechanisms involved in these cases differ from that proposed here, and with the activation enthalpy recently determined for a biomimetic catecholase reaction.[38] In Scheme 3, phenol hydroxylation is shown to occur by way of an electrophilic aromatic substitution mechanism, which is consistent with a recent investigation on tyrosinase activity towards simple *para*-substituted phenols.[39]

This rules out the possibility that the reaction proceeds through steps involving radical species, in agreement with experimental results.[40] A concerted pathway of O–O bond cleavage and C–O bond formation is assumed here to account for the overall larger energy barrier involved in the monophenolase reaction compared to the catecholase reaction. The concerted pathway is consistent with the small but non-negligible isotope effect observed on k_{cat} with 3,5-[D_2]-L-TyrOMe, which indicates that the C–H bond is involved in the formation of the activated complex. Small kinetic isotope effects, between 1 and 3, are not unusual in electrophilic aromatic substitutions,[41] and are generally due to a partitioning effect,[42] which involves reversibility in the formation of the intermediate. A solvent deuterium isotope effect

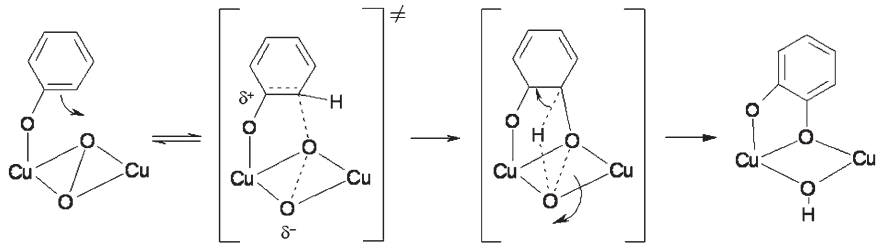

Scheme 3.

has also been found for tyrosinase reactions.[21,43] The effect was attributed to the transfer of a proton from the substrate hydroxyl group to the bound peroxide, but it is actually more difficult to rationalize, because the solvent k^H/k^D values do not correlate with the substrate acidity or the electron density at the aromatic carbon bearing the hydroxyl group. In addition, the effect of the deuterated buffer on the enzyme structure was not assessed. The absence of isotope effect found for the enzymatic oxidation of *p*-chlorophenol by hydrogen peroxide[26] may be related to the stronger acidity of the hydrogen *ortho* to the OH group due to the electron-withdrawing effect of the Cl. In a very recent study on a model complex, cleavage of the μ-peroxo O–O bond to generate the bis(μ-oxo) form was shown to occur before phenol hydroxylation.[44] The possibility that in the protein a bis(μ-oxo)dicopper(III) complex, rather than the usually assumed μ-peroxodicopper(II) isomer, might be the active species in the phenol hydroxylation is intriguing, but is inconsistent with the isotope effect found here for tyrosinase.

Regarding the activation entropy term for the phenol hydroxylation, a negative value is expected for the evolution of the ternary complex to the transition state, because the phenolate residue is strongly immobilized upon C–O bond formation. This is confirmed by the activation entropy data obtained from model studies on intramolecular aromatic hydroxylations of the endogenous ligands by peroxodicopper(II)[45] or hydroperoxodicopper(II)[46] complexes and, more recently, for the hydroxylation of an exogenous phenolate by a biomimetic peroxodicopper(II) complex.[47] The small $\Delta S^{\neq}$ term found here for the enzymatic monophenolase reaction implies a high level of preorganization in the active site of the enzyme. This indicates that very little structural rearrangement occurs upon cleavage of the O–O bond in the transition state.

The interpretation of the diphenolase reaction is complicated by the fact that cleavage of the peroxide bond involves coupled electron and proton transfers from the substrate,[30,37,38] and it is difficult to predict the sequence of events, since it is likely that protein residues at the active site, as well as ionizable groups on the substrate, participate as proton storage/delivery devices. Compared to the monophenolase reaction, proton transfers from the diphenol are greatly facilitated by its stronger acidity. As a matter of fact, the $\Delta S^{\neq}$ term shows opposite sign with dopamine and L-Dopa, although its value remains rather small. In a recently studied model catecholase reaction, a large and positive value of $\Delta S^{\neq}$ was found,[38] although in this case the substrate possessed two bulky *tert*-butyl substituents on the catechol ring, which most probably caused excessive crowding in the ternary complex. This crowding would have been relieved upon cleavage of the O–O bond and release of the quinone product. We can thus formulate the evolution of the ternary complex involved in Equation (9) according to the two alternative routes represented in Scheme 4 and Scheme 5, depending on whether proton transfer from bound catecholate occurs before or after O–O bond cleavage. Energetic considerations suggest that the two pathways should be essentially equivalent, since proton transfers involve a small energy barrier and heterolytic cleavages of peroxo or hydroperoxo O–O bonds are expected to be similar in energy.[15,37]

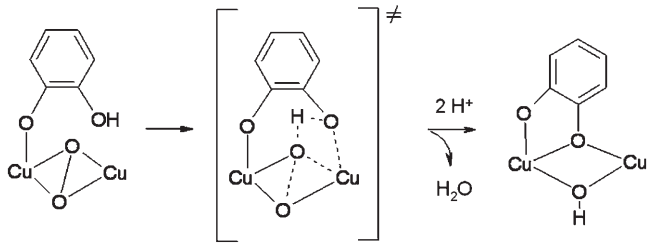

Scheme 4.

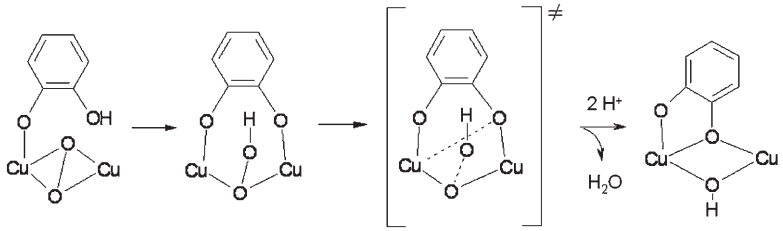

Scheme 5.

Assuming that the substrates bind to tyrosinase in a fast pre-equilibrium step, the Michaelis constants give information on the affinities for the enzyme active species. In general, when differences in steric effects are minimized, the affinity of the substrate has been shown to correlate with the electron density on the phenol.[48] The thermodynamics of substrate binding provides some further useful information about the type of interaction occurring at the active site. In all cases, the tyrosinase–substrate binding interaction is enthalpy driven (Table 2). This seems to be a general characteristic of enzyme-substrate complexes involving polar phenolic and diphenolic compounds, as has been shown for peroxidases.[27,28] In the present case, the binding enthalpies are indeed large, probably because, compared to the peroxidase complexes with simple phenols, the polar groups on the side chains of the substrates studied here give rise to additional electrostatic or hydrogen-bonding interactions with suitable amino acid residues in the tyrosinase active site. In addition, the polar interactions with peroxidases involving the phenol hydroxyl groups are replaced here by covalent Cu^{II}–phenolate or Cu^{II}–catecholate bonds. In the case of both peroxidases[28] and tyrosinase,[14,21] it is usually assumed that the aromatic nucleus of the substrate is involved in hydrophobic, ring-stacking interactions with an aromatic residue, but on energetic grounds this contribution is overwhelmed by polar interactions. The large and negative binding entropy terms

in Table 2 are also characteristic of protein-substrate interactions dominated by polar interactions,[27,28] reflecting more ordered states in the protein complexes. In the present case, we also have to take into account the fact that substrate binding occurs to the oxy form of the protein (reactions according to [Eq. (8)] and [Eq. (9)]), producing a somewhat crowded ternary complex. The difference between the binding parameters for monophenols and diphenols might be associated with the view that in the first case the binding occurs to the Cu_A center and in the second case to the Cu_B center of the enzyme.[36] However, cw-EPR experiments on half-met-tyrosinase adducts with *p*-nitrophenol and kojic acid show that binding always occurs to the oxidized copper, suggested to be Cu_B.[16] When nonpolar, hydrophobic effects dominate protein-substrate interactions, the situation is completely different. For instance, binding of camphor to *P. Putida* cytochrome P450 occurs with $\Delta H^\circ = 0$ and $\Delta S^\circ = +110\,J\,K^{-1}\,mol^{-1}$,[49] and binding of benzphetamine to human CYP2B4 occurs with $\Delta H^\circ = +29.3\,kJ\,mol^{-1}$ and $\Delta S^\circ = +170\,J\,K^{-1}\,mol^{-1}$,[50,51] that is, both processes are strongly entropy driven. In the latter case, the major contribution to the binding free energy is due to desolvation of the active site upon substrate binding, which is relatively large, while polar (hydrogen bonding/electrostatic) contributions are very limited. The thermodynamic data for inhibitor binding to tyrosinase are fully consistent with the above arguments, even though in this case the binding involves the met form of the protein. Compare, for instance, the parameters for binding of benzoic acid and toluene to mushroom tyrosinase: $\Delta H^\circ_I = -134\,kJ\,mol^{-1}$ and $\Delta S^\circ_I = -356\,J\,K^{-1}\,mol^{-1}$ as opposed to $\Delta H^\circ_I = +54\,kJ\,mol^{-1}$ and $\Delta S^\circ_I = +226\,J\,K^{-1}\,mol^{-1}$, respectively.[21] As we noted above, the ΔH°_I and ΔS°_I terms for benzoic acid binding resemble the exceedingly large and negative binding parameters that we have found for the anomalous substrate Hpp (Table 2).

The inhibitory effect of carboxylic acids on tyrosinase has been known for a long time.[21,29] Therefore, it is somewhat surprising to note that the reported activity of the enzyme towards phenolic acids such as Hpp is not different from that observed for related phenolic substrates lacking the carboxylate function or bearing an amino group at the α-carbon, as is the case in tyrosine.[19] The temperature dependence of the enzyme activity studied here reveals the anomalous behavior with this particular type of substrate, for which there is competitive binding to the enzyme through the phenol or carboxylate groups. The presence of an amino group at the C_α atom of the side chain in the substrate apparently prevents the latter possibility. At room temperature, fast equilibration of the two binding modes enables the apparent normal behavior of Hpp as a substrate, and it actually becomes highly reactive at higher temperatures, probably because its negative charge makes the phenol nucleus more electron-rich. On lowering the temperature, however, the effect of the large exothermic inhibition term becomes dominant. This effect exceeds the usual decrease in enzyme activity on lowering the temperature.

If the hypothesis of slow substrate binding due to Garcia-Canovas were valid,[30] the parameters obtainable from the temperature dependence of the rates would not be ΔH° and ΔS° but the activation parameters for substrate binding, $\Delta H^{\neq}_{on}$ and $\Delta S^{\neq}_{on}$. The data reported in Table 2 show very low $\Delta H^{\neq}_{on}$ values for phenolic substrates. These low values cannot be simply attributed to the susceptibility to ligand substitution of copper(II) ions, since similar values should then be observed with catechols. Furthermore, ligand substitutions in copper(II) model complexes are associated with much larger activation enthalpies, ranging from 25 to 85 $kJ\,mol^{-1}$, depending on the complex and the reaction conditions.[52–54] Therefore, at least for phenolic substrates, the hypothesis of slow binding to tyrosinase is unlikely. The $\Delta H^{\neq}_{on}$ values reported in Table 2 for dopamine and L-Dopa could be consistent with the slow substrate binding hypothesis,[30] but this is contradicted by NMR relaxation data pertaining to the binding of inhibitors at the enzyme, especially the catechol-like kojic acid (Figure 6), which show that this process is always fast.

Conclusions

In conclusion, tyrosinase functions in the aqueous/organic solvent used in the present study with only minor alterations of catalytic efficiency compared to in an aqueous solution. There is no evidence that the cryosolvent alters the fundamental nature of the enzymatic reactions and therefore the kinetic activation parameters derived from the variable-temperature study reflect the intrinsic features of the evolution of the transition states. The findings that 1) the activation free energy is essentially determined by cleavage of the peroxide O–O bond, and 2) the $\Delta S^{\neq}$ term is small, are fully consistent with the view that the enzyme environment must be preorganized to be complementary to the transition state configuration of the reactants.[55,56] This is particularly important for the monophenolase reaction, in which the substrate undergoes an energetically demanding C–H bond cleavage process. The strikingly anomalous behavior of Hpp can be fully rationalized by a kinetic model that takes into account the dual substrate/inhibitor nature of this compound.

The evidence from the substrate binding data indicates that the active site of tyrosinase is polar. However, a large portion of the substrate binding energy involves interactions of the polar groups on the side chain, far from the reaction site on the phenolic or diphenolic nucleus. This is confirmed by the substrate stereospecificity exhibited by tyrosinase, whereby replacing L-tyrosine with D-tyrosine or L-Dopa with D-Dopa affects only K_M and not k_{cat} of the enzymatic reaction.[57] In addition, as shown by model studies on the monophenolase reaction employing a dinuclear copper complex, phenol binding to the peroxodicopper(II) species appears to be weak.[47] Therefore, the polar interactions essentially responsible for enzyme catalysis must involve preoriented protein dipoles capable of stabilizing the development of charges in the transition state (Scheme 3), in agreement with the

current understanding of the origin of enzyme catalysis.[56,58] The results described here provide a rationale for the planning of further experiments that will allow direct scrutiny of the key intermediates of the tyrosinase catalytic cycles by low-temperature spectroscopy in the aqueous/organic medium investigated.

Experimental Section

Reagents: Tyramine, L-tyrosine, L-tyrosine methyl ester hydrochloride, *N*-acetyl-L-tyrosine, Hpp, L-Dopa hydrochloride, and kojic acid were obtained from Aldrich. 3,5-[D_2]-L-Tyrosine (99.2 atom % D) was obtained from CDN isotopes. All the other chemicals were of analytical grade and were used as received. 3,5-[D_2]-L-Tyrosine methyl ester hydrochloride was prepared by esterification of 3,5-[D_2]-L-tyrosine according to the following procedure. A stream of dry hydrogen chloride gas was passed through a solution of 3,5-[D_2]-L-tyrosine (0.5 g) in dry methanol (10 mL) for 0.5 h. The solution was then gently heated at reflux for 3 h. After cooling, the solution was concentrated to dryness in vacuo. Recrystallization of the oily residue from ethanol/diethyl ether gave the final product (yield 90 %). The ^{1}H NMR spectrum of the product, recorded in D_2O on a Bruker AVANCE 400 spectrometer, showed that the esterification had occurred with a partial loss of isotopic enrichment, to a final 90.1 atom % D.

To determine the exact pH of the mixed aqueous/organic solvent, a glass electrode was calibrated by the addition of measured quantities of a standard perchloric acid solution to a 34.4 % methanol–glycerol (7:1, v/v) and 65.6 % (v/v) water solution at the desired temperature according to Gran's method.[59] The temperature dependence of the buffer pH was found to be very small; for instance, between the temperatures of 25 and 10 °C the pH changed from 6.74 to 6.96. Therefore, the pH changes with temperature were neglected.

Enzyme preparation: Mushroom tyrosinase (3960 units mg^{-1}) was obtained from Sigma and was purified according to the procedure of Duckworth and Coleman.[60] To rule out the presence of any enzymatic activity not related to tyrosinase, a 10 % native-PAGE was run and then split into two parts that were respectively stained with Coomassie Brilliant Blue, to identify proteins, and with a substrate to highlight enzymatic activity. The reaction mixture for the zymogram had the following composition: 1 mM L-Dopa, 8 mM MBTH, 4 % DMF in 100 mM phosphate buffer at pH 7.0, and the staining reaction was carried out for 10 min at 37 °C. This assay showed that the small amounts of protein impurities were completely inactive in L-Dopa oxidation. The enzyme concentration was calculated from the reported activity of the purified enzyme in the L-tyrosine oxidation assay[23] and assuming a molecular mass of 120 kDa.[19]

Kinetics: The catalytic oxidation of L-Dopa, dopamine, tyramine, L-TyrOMe, 3,5-[D_2]-L-TyrOMe, Hpp, and *N*-acetyl-L-tyrosine was studied in the mixed solvent of 34.4 % methanol/glycerol (7:1, v/v) and 65.6 % (v/v) aqueous 50 mM Hepes buffer at pH 6.8, saturated with atmospheric oxygen. The kinetic experiments were followed spectrophotometrically using a magnetically stirred, thermostatted, 1-cm pathlength cell and an HP8452 A diode-array spectrophotometer for temperatures above 8 °C. The experiments at lower temperatures were performed using a custom-designed immersible fiber-optic quartz probe (5 mm pathlength, Hellma). The temperatures were controlled to within ± 0.1 °C using a Haake cryostat with circulating fluid and directly checked inside the solution with a thermometer with a precision of ± 0.1 °C.

The formation of the dopachrome derivatives of L-Dopa, dopamine, tyramine, L-TyrOMe, and 3,5-[D_2]-L-TyrOMe was followed through the increase of the characteristic dopachrome absorption band at 476 nm. The extinction coefficients of the various dopachrome derivatives were assumed to be equal to that of L-Dopa, that is, 3600 $M^{-1}cm^{-1}$; the effect of the cryosolvent on the intensity and position of the absorption maxima of the dopachrome derivatives was taken to be negligible. To decrease the effect of noise on the absorbance reading during the kinetic determinations, it was convenient to monitor the difference between the absorbance at 476 nm and that at 800 nm, at which the absorbance remains negligible during the assay.

The rate dependence on [L-Dopa] and on [dopamine] was determined by varying the substrate concentration from 0.0 to 8.0 mM and from 0.0 to 3.0 mM, respectively, using a tyrosinase concentration of 12.5 nM. The temperature dependences of the rates were studied in the ranges 2.0–28.0 °C and 0.0–28.0 °C, respectively. The rates in units of $\Delta A\,s^{-1}$ were calculated from the slopes of the traces at 476 nm in the first 20–25 s after mixing of the reagents; the conversion from units of $\Delta A\,s^{-1}$ to s^{-1} was made using the dopachrome extinction coefficient and the tyrosinase concentration.

The dependence of the rate of L-Dopa oxidation as a function of the concentration of the organic component of the cryosolvent was studied at 8 °C by varying the amount of methanol–glycerol (7:1, v/v) contained in aqueous 50 mM Hepes buffer at pH 6.8, saturated with atmospheric oxygen. The concentration range of the organic component analyzed was from 0 to 42.5 % (v/v). The L-Dopa concentration was varied from 1 to 21 mM, while the concentration of tyrosinase was 35 nM.

The rate dependence on [tyramine], [L-TyrOMe], and [3,5-[D_2]-L-TyrOMe] was determined in the concentration range from 0.0 mM to about 4.2 mM. In order to reduce the lag phase of the reaction and to increase the linear portion of the rate versus [substrate] plot, the kinetic experiments were performed by adding a constant amount (1 μM) of L-Dopa as the first reagent. The rate data for 3,5-[D_2]-L-TyrOMe were corrected for 90 % isotopic enrichment. The temperature dependence of the rate was studied in the range 9.0–28.0 °C for tyramine and in the range 8.0–28.0 °C for L-TyrOMe. The rates in units of $\Delta A\,s^{-1}$ were calculated from the slopes of the traces at 476 nm in the time interval over which the greatest slope of the curve was observed. The reactions were followed for 12 min.

The rate dependence on [Hpp] was determined in the concentration range from 0.0 mM to 9.0 mM. The temperature dependence of the rate was studied in the range 8.0–25.0 °C. The enzymatic oxidation of this substrate gave a relatively stable *o*-quinone and enzyme activity was determined by monitoring the absorption of the *o*-quinone at 396 nm (ε = 1200 $M^{-1}cm^{-1}$). At temperatures above 25 °C, however, the transformation of the quinone into the dopachrome became non-negligible, preventing an accurate determination of the rate data. In order to reduce the lag time and to increase the linear portion of the curve, the kinetic experiments were performed by adding a constant amount (2 μM) of L-Dopa as the first reagent. The rates in units of $\Delta A\,s^{-1}$ were calculated from the slopes of the traces at 396 nm over the appropriate time intervals, usually in the range 600–800 s. The kinetic parameters k_{cat} and K_M were obtained by fitting of the rate *vs.* [substrate] plots.

The tyrosinase activity in the oxidation of *N*-acetyl-L-tyrosine was very low; therefore, for this substrate the determination of k_{cat} and K_M in the usual temperature range was not possible.

NMR experiments: The NMR T_1 relaxation times for the protons of kojic acid in the presence of variable amounts of tyrosinase were determined at 25 °C by the standard inversion recovery method.[61] A solution of kojic acid was prepared in deuterated 50 mM sodium phosphate buffer at pD 6.8. In order to eliminate interferences by traces of metal ion impurities, a small amount of EDTA was added to the solution. Tyrosinase samples were prepared by dissolving the lyophilized enzyme in 50 mM sodium phosphate buffer at pH 6.8. The enzyme solution was dialyzed against 1 mM EDTA in 50 mM sodium phosphate buffer at pH 6.8 and then against milliQ water. The enzyme was then lyophilized and redissolved in D_2O. The tyrosinase concentration of this solution (0.28 mM) was calculated from its activity as described above. The concentrations employed in the experiments were as follows: [kojic acid] 10.0 mM, [tyrosinase] from 0 to 12.5 μM. The paramagnetic relaxation rate of the protons of kojic acid interacting with tyrosinase, T_{1b}, was calculated from the experimental relaxation rate, T_{1obs}, using Equation (10),[32]

$$\frac{1}{T_{1obs}} = \frac{1}{T_{1f}} + \frac{E_0}{S + K_D}\left(\frac{1}{T_{1b}} - \frac{1}{T_{1f}}\right) \qquad (10)$$

where T_{1f} is the T_1 value for free inhibitor, E_0 and S are the enzyme and kojic acid concentrations, respectively, and K_D, assumed to be equal to the inhibition constant $K_I = 30\ \mu M$,[31] is the dissociation constant for the tyrosinase-kojic acid complex.

Acknowledgements

This work was supported by the Italian MIUR, through a PRIN project (Progetto di Rilevante Interesse Nazionale), and by the University of Pavia. The support and sponsorship provided by COST Action D21 "Metalloenzymes and Chemical Biomimetics" is kindly acknowledged. The C.I.R.C.M.S.B. is gratefully acknowledged for a fellowship to A.G.

[1] H. S. Mason, *Annu. Rev. Biochem.* **1965**, *34*, 595–634.
[2] J. N. Rodriguez-Lopez, L. G. Fenoll, M. J. Peñalver, P. A. Garcia-Ruiz, R. Varon, F. Martinez-Ortiz, F. Garcia-Canovas, J. Tudela, *Biochim. Biophys. Acta* **2001**, *1548*, 238–256.
[3] E. J. Land, C. A. Ramsden, P. A. Riley, *Acc. Chem. Res.* **2003**, *36*, 300–308.
[4] E. I. Solomon, U. M. Sundaram, T. E. Machonkin, *Chem. Rev.* **1996**, *96*, 2563–2605.
[5] E. Jaenicke, H. Decker, *ChemBioChem* **2004**, *5*, 163–169.
[6] E. I. Solomon, P. Chen, M. Metz, S.-K. Lee, A. E. Palmer, *Angew. Chem.* **2001**, *113*, 4702–4724; *Angew. Chem. Int. Ed.* **2001**, *40*, 4570–4590.
[7] K. Magnus, B. Hazes, H. Ton-That, C. Bonaventura, J. Bonaventura, W. Hol, *Proteins* **1994**, *19*, 302–309.
[8] M. E. Cuff, C. Miller, K. E. van Holde, W. A. Hendrickson, *J. Mol. Biol.* **2000**, *278*, 855–870.
[9] T. Klabunde, C. Eicken, J. C. Sacchettini, B. Krebs, *Nat. Struct. Biol.* **1998**, *5*, 1084–1090.
[10] L. Bubacco, J. Salgado, E. Vijgenboom, G. W. Canters, *FEBS Lett.* **1999**, *442*, 215–222.
[11] H. Decker, T. Rimke, *J. Biol. Chem.* **1998**, *273*, 25889–25892.
[12] H. Decker, M. Ryan, E. Jaenicke, N. Terwilliger, *J. Biol. Chem.* **2001**, *276*, 17796–17799.
[13] C. Gerdemann, C. Eicken, B. Krebs, *Acc. Chem. Res.* **2000**, *33*, 183–191.
[14] H. Decker, R. Dillinger, F. Z. Tuczek, *Angew. Chem.* **2000**, *112*, 1656–1660; *Angew. Chem. Int. Ed.* **2000**, *39*, 1591–1595.
[15] P. E. M. Siegbahn, *J. Biol. Inorg. Chem.* **2003**, *8*, 567–576.
[16] L. Bubacco, M. van Gastel, E. J. J. Groenen, E. Vijgenboom, G. W. Canters, *J. Biol. Chem.* **2003**, *278*, 7381–7389.
[17] A. W. J. W. Tepper, L. Bubacco, G. W. Canters, *J. Am. Chem. Soc.* **2005**, *127*, 567–575.
[18] T. Plenge, R. Dillinger, L. Santagostini, L. Casella, F. Z. Tuczek, *Z. Anorg. Allg. Chem.* **2003**, *629*, 2258–2265.
[19] J. C. Espin, R. Varon, L. G. Fenoll, M. A. Gilabert, P. A. Garcia-Ruiz, J. Tudela, F. Garcia-Canovas, *Eur. J. Biochem.* **2000**, *267*, 1270–1279.
[20] L. G. Fenoll, M. J. Peñalver, J. N. Rodriguez-Lopez, P. A. Garcia-Ruiz, F. Garcia-Canovas, J. Tudela, *Biochem. J.* **2004**, *380*, 643–650.
[21] J. S. Conrad, S. R. Dawso, E. R. Hubbard, T. E. Meyers, K. G. Strothkamp, *Biochemistry* **1994**, *33*, 5739–5744.
[22] V. Réat, J. L. Finney, A. Steer, M. A. Roberts, J. Smith, R. Dunn, M. Peterson, R. Daniel, *J. Biochem. Biophys. Methods* **2000**, *42*, 97–103.
[23] A. Rescigno, E. Sanjust, G. Soddu, A. C. Rinaldi, F. Sollai, N. Curreli, A. Rinaldi, *Biochim. Biophys. Acta* **1998**, *1384*, 268–276.
[24] K. J. Liu, M. W. Grinstaff, J. Jiang, K. S. Suslick, H. M. Swartz, W. Wang, *Biophys. J.* **1994**, *67*, 896–901.
[25] J. N. Rodriguez-Lopez, L. G. Fenoll, P. A. Garcia-Ruiz, R. Varon, J. Tudela, R. N. F. Thorneley, F. Garcia-Canovas, *Biochemistry* **2000**, *39*, 10497–10506.
[26] S. Yamazaki, C. Morioka, S. Itoh, *Biochemistry* **2004**, *43*, 11546–11553.
[27] K.-G. Paul, P.-I. Ohlsson, *Acta Chem. Scand.* **1978**, *B32*, 395–404.
[28] S. Modi, D. V. Behere, S. Mitra, *Biochim. Biophys. Acta* **1989**, *996*, 214–225.
[29] D. E. Wilcox, A. G. Porras, Y. T. Hwang, K. Lerch, M. E. Winkler, E. I. Solomon, *J. Am. Chem. Soc.* **1985**, *107*, 4015–4027.
[30] J. R. Ros, J. N. Rodriguez-Lopez, F. Garcia-Canovas, *Biochim. Biophys. Acta* **1994**, *1204*, 33–42.
[31] J. S. Chen, C. I. Wei, R. S. Rolle, W. S. Otwell, M. O. Balaban, M. R. Marshall, *J. Agric. Food Chem.* **1991**, *39*, 1396–1401.
[32] L. Banci, I. Bertini, C. Luchinat, *Nuclear and Electron Relaxation. The Magnetic Nucleus-Unpaired Electron Coupling in Solution*, VCH, Weinheim, **1991**.
[33] A. Zaks, A. M. Klibanov, *J. Biol. Chem.* **1988**, *263*, 8017–8021.
[34] G. M. Jacobsohn, R. Iskander, M. K. Jacobsohn, *Biochim. Biophys. Acta* **1993**, *1202*, 317–324.
[35] S. Kermasha, H. Bao, B. Bisakowski, *J. Mol. Catal. B* **2001**, *11*, 929–938.
[36] C. Olivares, J. C. Garcia-Borròn, F. Solano, *Biochemistry* **2002**, *41*, 679–686.
[37] P. E. M. Siegbahn, *J. Biol. Inorg. Chem.* **2004**, *9*, 577–590.
[38] A. Granata, E. Monzani, L. Casella, *J. Biol. Inorg. Chem.* **2004**, *9*, 903–913.
[39] S. Yamazaki, S. Itoh, *J. Am. Chem. Soc.* **2003**, *125*, 13034–13035.
[40] R. P. Ferrari, E. Laurenti, E. M. Ghibaudi, L. Casella, *J. Inorg. Biochem.* **1997**, *68*, 61–69.
[41] M. B. Smith, J. March, *March's Advanced Organic Chemistry, 5th ed.*, Wiley, New York, **2001**, Chapter 11.
[42] L. P. Hammett, *Physical Organic Chemistry, 2nd ed.*, McGraw-Hill, New York, **1970**, p. 172.
[43] L. G. Fenoll, M. J. Peñalver, J. N. Rodriguez-Lopez, P. A. Garcia-Ruiz, F. Garcia-Canovas, J. Tudela, *Biochem. J.* **2004**, *380*, 643–650.
[44] L. M. Mirica, M. Vance, D. J. Rudd, B. Hedman, K. O. Hodgson, E. I. Solomon, T. D. P. Stack, *Science* **2005**, *308*, 1890–1892.
[45] K. D. Karlin, A. D. Zuberbühler, *Bioinorganic Catalysis, 2nd ed.* (Eds.: J. Reedijk, E. Bowman), Dekker, New York, **1999**, pp. 469–534.
[46] G. Battaini, E. Monzani, A. Perotti, C. Para, L. Casella, L. Santagostini, M. Gullotti, R. Dillinger, C. Näther, F. Tuczek, *J. Am. Chem. Soc.* **2003**, *125*, 4185–4198.
[47] S. Palavicini, A. Granata, E. Monzani, L. Casella, *J. Am. Chem. Soc.*, in press.
[48] G. Battaini, E. Monzani, L. Casella, E. Lonardi, A. W. J. W. Tepper, G. W. Canters, L. Bubacco, *J. Biol. Chem.* **2002**, *277*, 44606–44612.
[49] B. W. Griffin, J. A. Peterson, *Biochemistry* **1972**, *11*, 4740–4746.
[50] K. Ruckpaul, H. Rein, J. Blanck, *Front. Biotransform.* **1989**, *1*, 1–65.
[51] D. F. V. Lewis, P. J. Eddershaw, M. Dickins, M. H. Tarbit, P. S. Goldfarb, *Chem.-Biol. Interact.* **1998**, *115*, 175–199.
[52] H. Voss, K. J. Wannovius, H. Elias, *Inorg. Chem.* **1979**, *18*, 1454–1459.
[53] F. Thaler, C. D. Hubbard, F. W. Heinemann, R. van Eldik, S. Schindler, I. Fabian, A. M. Dittler-Klingemann, F. E. Hahn, C. Orvig, *Inorg. Chem.* **1998**, *37*, 4022–4029.
[54] A. Neubrand, F. Thaler, M. Körner, A. Zahl, C. D. Hubbard, R. van Eldik, *J. Chem. Soc. Dalton Trans.* **2002**, 957–961.
[55] W. R. Cannon, S. J. Benkovic, *J. Biol. Chem.* **1998**, *273*, 26257–26260.
[56] A. Warshel, *J. Biol. Chem.* **1998**, *273*, 27035–27038.
[57] J. C. Espin, P. A. Garcia-Ruiz, J. Tudela, F. Garcia-Canovas, *Biochem. J.* **1998**, *331*, 547–551.
[58] J. Villà, M. Štrajbl, T. M. Glennon, Y. Y. Sham, Z. T. Chu, A. Warshel, *Proc. Natl. Acad. Sci. USA* **2000**, *97*, 11899–11904.
[59] F. J. C. Rossotti, H. J. Rossotti, *J. Chem. Educ.* **1965**, *42*, 375–378.
[60] H. W. Duckworth, J. E. Coleman, *J. Biol. Chem.* **1970**, *245*, 1613–1625.
[61] R. L. Vold, J. S. Waugh, M. P. Klein, D. E. Phelps, *J. Chem. Phys.* **1968**, *48*, 3831–3832.

Received: September 5, 2005
Published online: December 8, 2005

